Single-polarization fiber-optic resonator for gyro applications

Robert P. Dahlgren & Robert E. Sutherland
617-258-1158
Charles Stark Draper Laboratory, Inc.
555 Technology Square, Cambridge, Massachusetts 02139

ABSTRACT

A novel fiber-optic resonant ring has been demonstrated that eliminates one of the orthogonal resonances in the cavity. Standard birefringent fiber resonators support two resonances, associated with the fast and slow eigenmodes of the resonator. The addition of an intercavity device increases the loss in one of the eigenmodes, thus squelching that resonance. We have fabricated resonant rings from birefringent fiber polished couplers with a length of polarizing fiber spliced into the cavity, which eliminates the orthogonal resonance, even for moderate amounts of subcomponent polarization cross-coupling. Resonators with deep, symmetric dips and with finesse of about 25 have been obtained, fabricated from adjustable and fixed polarization-maintaining couplers.

1. INTRODUCTION

High-finesse ring resonators have been fabricated successfully[1,2] and have applications in navigation and other fields. Single-mode and polarization-maintaining (PM) fiber resonators suffer from the fact that these fibers support two orthogonally polarized modes. This results in a pair of resonances, which can be of different order, corresponding to the orthogonal polarizations.[3] As environmental factors perturb the cavity, the resonances occasionally overlap[4] and exchange power. Large amounts of coupling can occur during resonance overlap due to phase matching, even for assemblies with a high degree of polarization isolation. To avoid this problem, it has been suggested[5,6] that a lossy element be included within the cavity to extinguish one of the ring resonances. Only a few dB of loss would be sufficient to spoil the Q of one of the resonant polarization states, producing a single-eigenstate-of-polarization (SEOP) resonator.

The first demonstration of this technique was a spliceless ring made completely from single-polarization (SP) PANDA fiber. Unfortunately, SP fiber does not lend itself to coupler fabrication due to the high stress levels and close proximity of the stress-applying part (SAP) to the fiber core. Fabrication of couplers from SP fiber has been found to be very difficult, and reliability was a problem. Commercially-available spliceless rings had a finesse of 20-25, and occasionally exhibited highly asymmetric dips. An alternate approach to achieve SEOP was to incorporate a 90-deg splice in the fiber[7] or a polarization-selective coupler.[7,8] This paper describes a novel hybrid SP cavity made with a PM coupler formed by splicing a section of SP fiber into the cavity.

2. COUPLER FABRICATION

The fabrication process begins with cutting a narrow groove, having a 30-cm bend radius, in a 7740 Pyrex glass block. This is done with a numerically-controlled 3-axis cutting fixture, and IC dicing wheels.[9] The precision of the blades and 0.1-μm resolution of linear motion ensure that the groove dimensions are highly reproducible. By carefully dressing the blades and actively sensing surface contact, groove depth and width is controlled to ±2 μm. The final step is a ductile-mode grinding pass to ensure a highly polished groove surface to minimize fiber microbending.

A short length of the jacket material is removed from a length of Fujikura SM13P polarization-maintaining fiber, and the exposed cladding is carefully cleaned. The identification and alignment of the principal axes of the fiber are accomplished to better than ±1 deg using an elasto-optic method.[10] Once the principal axes have been identified and oriented, the fiber is lowered into the groove, taking care not to disturb the alignment. The fiber is oriented with the fast axis parallel to the polished surface such that one SAP is lapped away. A small amount of a specially formulated adhesive is wicked into the groove, followed by an oven cure process to firmly season the epoxy. Quality control of adhesive and half-coupler preparation is extremely important to obtain a reproducible polishing and assembly process.

 0-8194-0716-X/92/$4.00

The lapping and polishing procedure has become fairly routine after a long period of development and experimentation. The preliminary grind is done with a standard Aluminum Oxide mixture on a cast iron lap. Once the excess epoxy is lapped away and the fiber is exposed, the glass block is uniformly ground to a fine finish, to about 25 μm from the core. Subsequently, the polishing operation uses a Polytron polishing pad[11] to get away from the much-troubled pitch approach to polishing. Pressure, temperature, solution chemistry, and other factors are carefully controlled to obtain a uniform polishing rate without subsurface damage. Shortly after one SAP is polished away, the polishing depth is estimated by an optical-matching fluid test[12] using n = 1.464 oil. Nomarski and Mirau microscopy techniques greatly facilitate polishing and inspection. Polished surfaces have been realized to a degree of flatness of $\approx\lambda/15$ and a surface roughness of ≈20 Å rms over several square mm measured with a Zygo interferometer. The extremely close fit between groove and fiber increases flatness, minimizes adhesives in the device, and allows for control of fiber stacking height, which must be ≈100 Å above the block surface.

When two coupler halves have been successfully polished, the final assembly begins with a preliminary cleanup of both halves. The two half-couplers are assembled in a laminar flow hood after they have been thoroughly cleaned by an alcohol wipe method with a cotton swab.[13] This cleaning method is done under high magnification, with high-purity solvents and extracted swabs. A water-break-free test is then performed to ensure the cleanliness of the two halves. Once both half-couplers are carefully mated, preliminary alignment of the fibers is performed under high magnification in an alignment fixture.

Diffused white light is used to observe color fringes in between the half-couplers. The appearance of a centrally-symmetric, zero-order (silver to black) fringe pattern is indicative of whether the two halves will optical contact bond successfully.[14] For adjustable couplers, index-matching oil (n = 1.458) is wicked in between the half-couplers, which remain in the alignment fixture. The half-coupler flatness requirement is relaxed for adjustable couplers.

Fine tuning the fiber-to-fiber transverse and longitudinal alignment is accomplished by a hookup to an ELED source and dual detector. Usually, the preliminary visual alignment is adequate to produce an initial small coupling. The final alignment in the fixture is completed by arriving at the desired coupling ratio (CR). The optical contact bond (OCB) is initiated by applying a slight pressure to the top half of the coupler. If flatness, cleanliness, and smoothness are sufficient, Van der Waals and other surface forces effectively attach the two half-couplers, which is manifested as a sudden change of the color fringes to transparency. As OCB begins, the preload adjustment screws are released, allowing the OCB region to further propagate over the entire area of the blocks. There is a small shift in CR during the bond, which can easily be compensated for. Incorrect CR can be corrected for by debonding with brief exposure to a heat gun. The OCB procedure is then repeated while precompensating for the CR shift. A permanent OCB usually forms over a 1-week period.[15] The data for the couplers in the experiment are listed in Table 1 for one adjustable coupler and one fixed coupler.

Table 1. Coupler performance.

	Variable	Coupler #1	Coupler #2
Type		Variable	OCB
Coupling ratio	κ^2	0 - 90 %	92 %
Loss	$L_{coupler}$	-0.1 dB	<< -0.1 dB
Cross-Coupling	10 log C	-22 dB	-17 dB

To date, this process has been successfully achieved time after time. The repetition of this process is owed mainly to the precision of the groove and the polishing fixture.

3. COIL FABRICATION

The coils were wound onto a 77-mm diameter aluminum coilform with low tension to minimize microbending. The coil consisted of 25 m of Fujikura SM13P-P polarizing PANDA fiber[16] wound in two layers. At that bending diameter, the fiber experiences attenuation of the fast eigenmode ≈-1.7 dB/m, and ≈-0.007 dB/m corresponding to the slow axis. The h-parameter is given by the vendor to be $\approx 10^{-6}$/m (for ideally benign conditions at a large bending diameter). The coils were wound with

low tension (<10 g), and were annealed at 90°C to give the acrylate fiber jacket a new "memory." The predicted coil performance is listed in Table 2, along with the measured performance values for the two coils used for ring assembly.

Table 2. Coil performance.

	Predicted	Coil #1	Coil #2
Loss L_{slow}	-0.14 dB	-0.16 dB	-0.24 dB
Extinction	43 dB	>40 dB	>40 dB

Extinction, which is defined as the the difference between the total attenuation for the coil modes L_{slow} - L_{fast}, has a positive value. The extinction ratio can be somewhat less than expected due to the finite cross-coupling of the fiber.[17] In addition, our measurement was limited to ≈40 dB due to bulk optics imperfections and minor field components.[18]

4. RESONATOR ASSEMBLY

The assembly was performed on a Fujikura FSM-20PM splicer, operated in the passive Profile Alignment System mode. The arc and other fusion conditions have been adjusted to perform PM-to-PZ splicing. Typical splice performance is

L_{splice} ≈-0.1 dB C ≈ -34 dB B < -50 dB

C is the polarization cross-coupling due to misalignment; B is the backreflection, which is OTDR measurement limited. The finished PM-to-PZ splice is recoated with UV-cured acrylate on a recoating fixture.[19] Figure 1 shows two possible assembly configurations that differ in the optimum CR requirement.

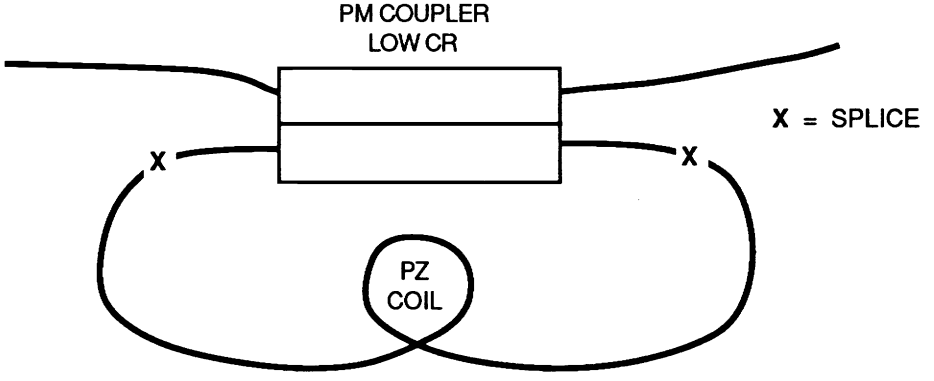

Figure 1a. Closed-loop topology.

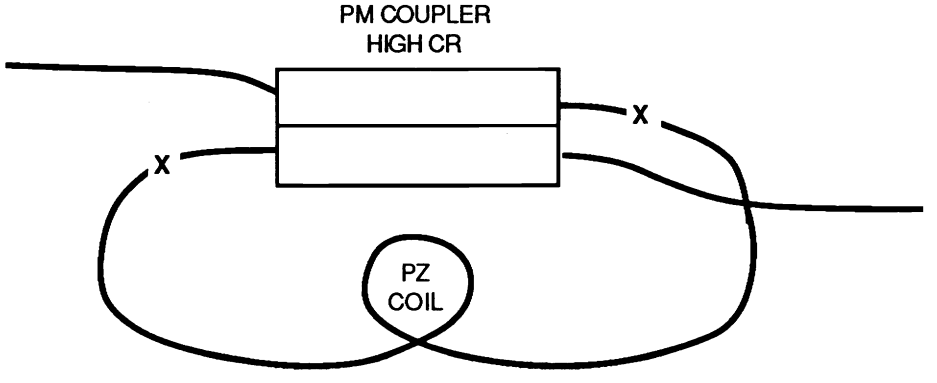

Figure 1b. Single-strand topology.

To minimize shot noise at the detector, it is desirable to have minimal ring output intensity when the laser is locked to a resonance. To maximize the dip depth parameter $\varepsilon^2 \equiv I_{min}/I_{max} << 1$, the coupler needs to be adjusted to the optimum intensity CR such that

$$\text{coupling out of cavity} + \text{cavity transmission} = 1$$

As κ^2 is adjusted to its optimum value κ^2_{opt} there is 100 percent dip depth and $\varepsilon^2 = 0$. Adding up coupler #1 loss, coil #1 loss, and predicted splice losses yield a sum of -0.46 dB. Calculating the loop intensity transmission ρ^2 from the total loss

$$\rho^2 \equiv 10^{0.1(L_{coupler}+L_{coil}+2\,L_{splice})} = 89.9\%$$

Recall that coupler #1 cannot be set to >90 percent CR, which leaves no safety margin if the splices were better than expected. To ensure that deep dips can be obtained, the closed-loop configuration must be used as shown in Figure 1a. The optimum coupling ratio is in this case much lower

$$1 - \kappa^2_{opt} = \rho^2$$

Thus, resonator #1 was assembled to form a closed-loop topology, with κ^2_{opt} = 10.1 percent; coupler #1 CR was easily readjusted to equal the losses.

Coupler #2 has a fixed CR κ^2 = 92.0 percent; thus, the single-strand topology will be used, as shown in Figure 1b. Due to the cavity configuration, one would now like the losses to be such that

$$\kappa^2_{opt} = \rho^2$$

In the case of resonator #2, loop losses are predicted to be -0.44 dB, or ρ^2 = 90.3 percent. For our fixed coupler, -0.36 dB would be optimum loop losses to achieve $\varepsilon^2 = 0$, requiring a splice loss of -0.06 dB.

The unattenuated eigenmode of the spliced resonator can be characterized[20] by the parameters (κ, ρ), where the amplitude CR defined as κ includes a 90° + δ phase shift. The dips are described by finesse f, ring asymmetry σ, and free-spectral range (FSR) defined as F ≡ c/nL. The relationship of these parameters for the case of no backscattering or polarization cross-coupling is given by

$$\kappa\rho = e^{-(\pi 1/f - i\sigma/F)} \qquad \text{and} \qquad \rho/\kappa = e^{-(\pi\varepsilon/f + i\sigma/F)}$$

For perfect ring symmetry (i.e., $\delta = 0$), the loss and coupling of the resulting cavity is calculated to be

$$\rho^2 = e^{-\pi(1/f + \varepsilon/f)} \qquad \text{and} \qquad \kappa^2 = e^{-\pi(1/f - \varepsilon/f)}$$

or, rearranging in terms of eigenmode parameters

$$\varepsilon = \frac{\ln\rho - \ln\kappa}{\ln\rho + \ln\kappa} \qquad f = \frac{-\pi}{\ln\rho + \ln\kappa}$$

The performances of the resonators were measured using a Nd:YAG nonplanar ring oscillator at λ = 1319 nm. The free-spectral range is measured by introducing a small sinusoidal phase modulation at a frequency near the FSR. As the modulation frequency is scanned, the FSR is read out in a method similar to Reference 21, but by direct observation of the dips rather than by generating the discriminant. To measure the linewidth of the resonator, the laser was swept by a slow

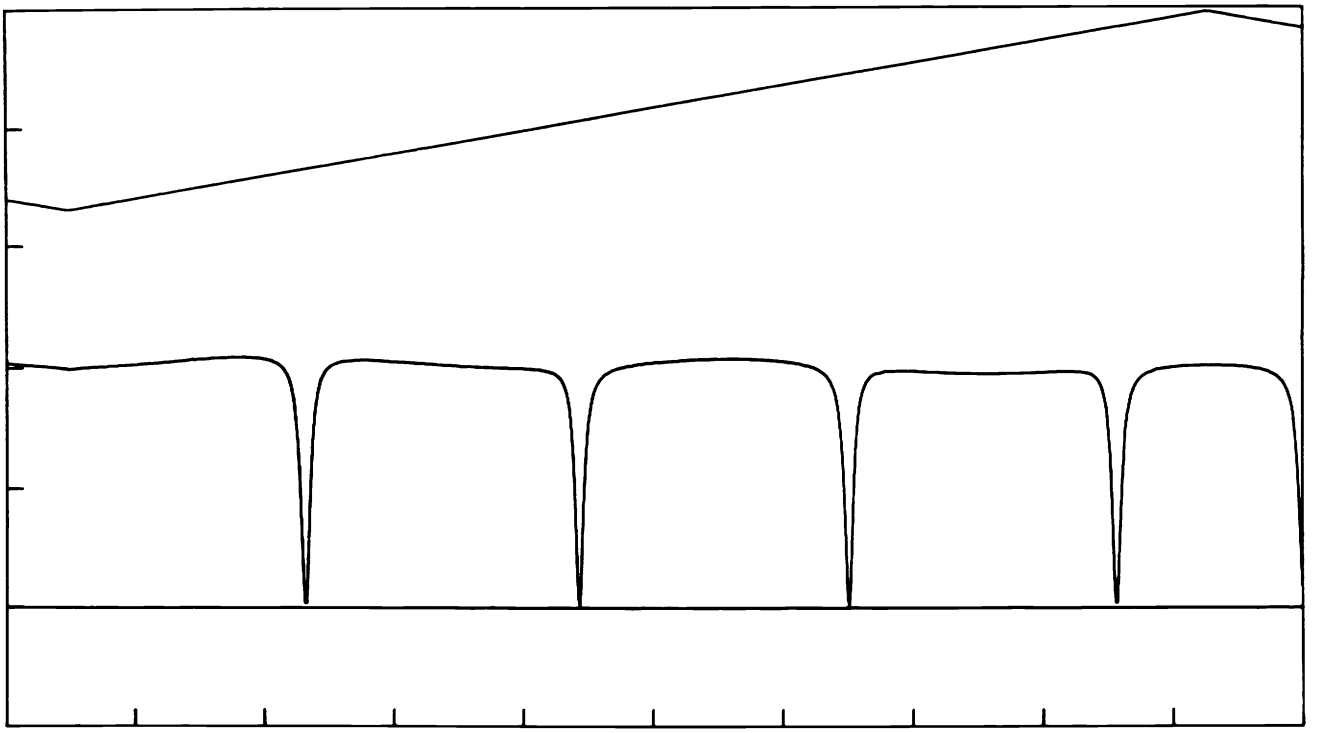

Figure 2. Adjustable resonator #1 transfer function.

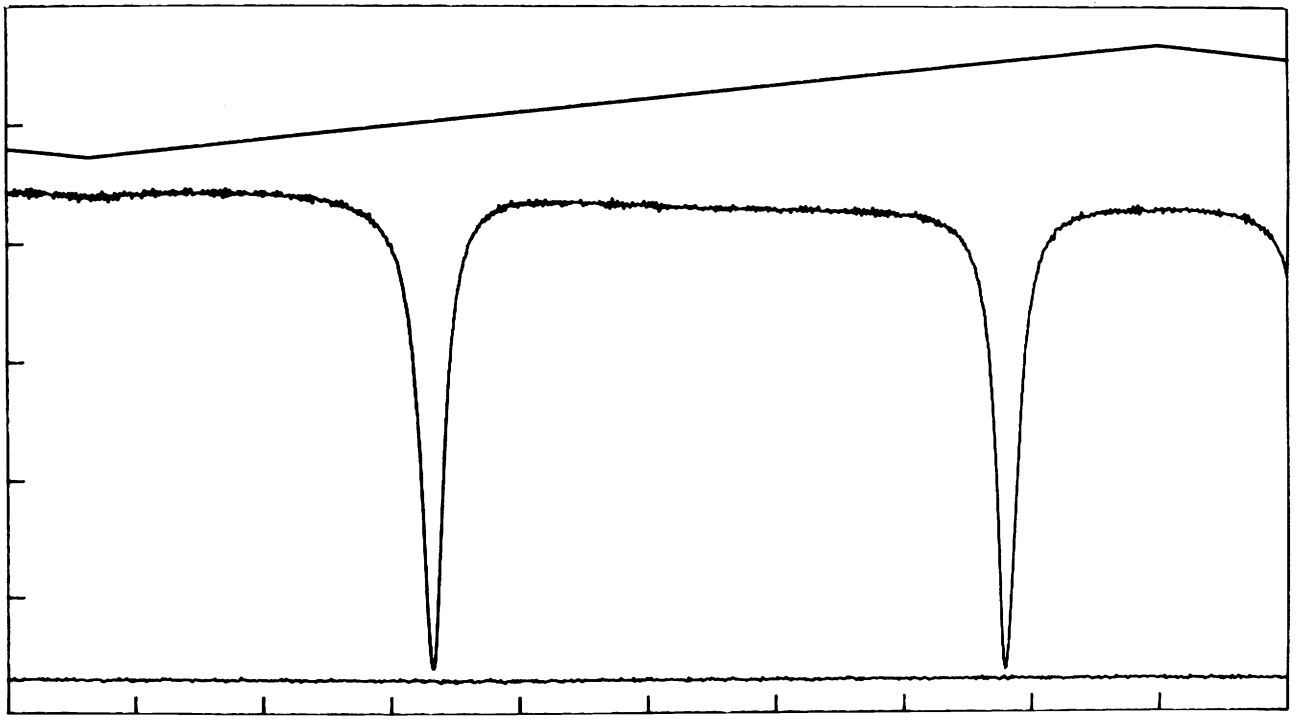

Figure 3. OCB resonator #2 transfer function.

triangle wave, and the resonator transfer function was captured by a digitizing oscilloscope. Finesse, dip depth, and extent of the orthogonal polarization dip were measured using the cursor functions of the scope.

Figure 2 shows the transfer function for resonator #1 with the CR adjusted to achieve minimum dips. Some of the asymmetry and sinusoidal modulation is due to parasitic Fabry-Perot modulation due to fiber end face reflection. Figure 3 shows the performance of assembly #2. Note the high degree of symmetry for this set of dips and the lack of any orthogonal polarization dips. The data is summarized in Table 3. Figure 4 shows a photograph of the OCB resonator.

Table 3. Resonator assembly performance.

	Variable	Ring #1	Ring #2
Type		Adjustable	Fixed
FSR	F	7.6 MHz	8.1 MHz
Finesse	f	27	25
Dip depth	ε^2	2 %	2%
Estimated loss	10 log ρ^2	-0.58 dB	-0.62 dB
Cross-Coupling	10 log C	<-30 dB	<-30 dB

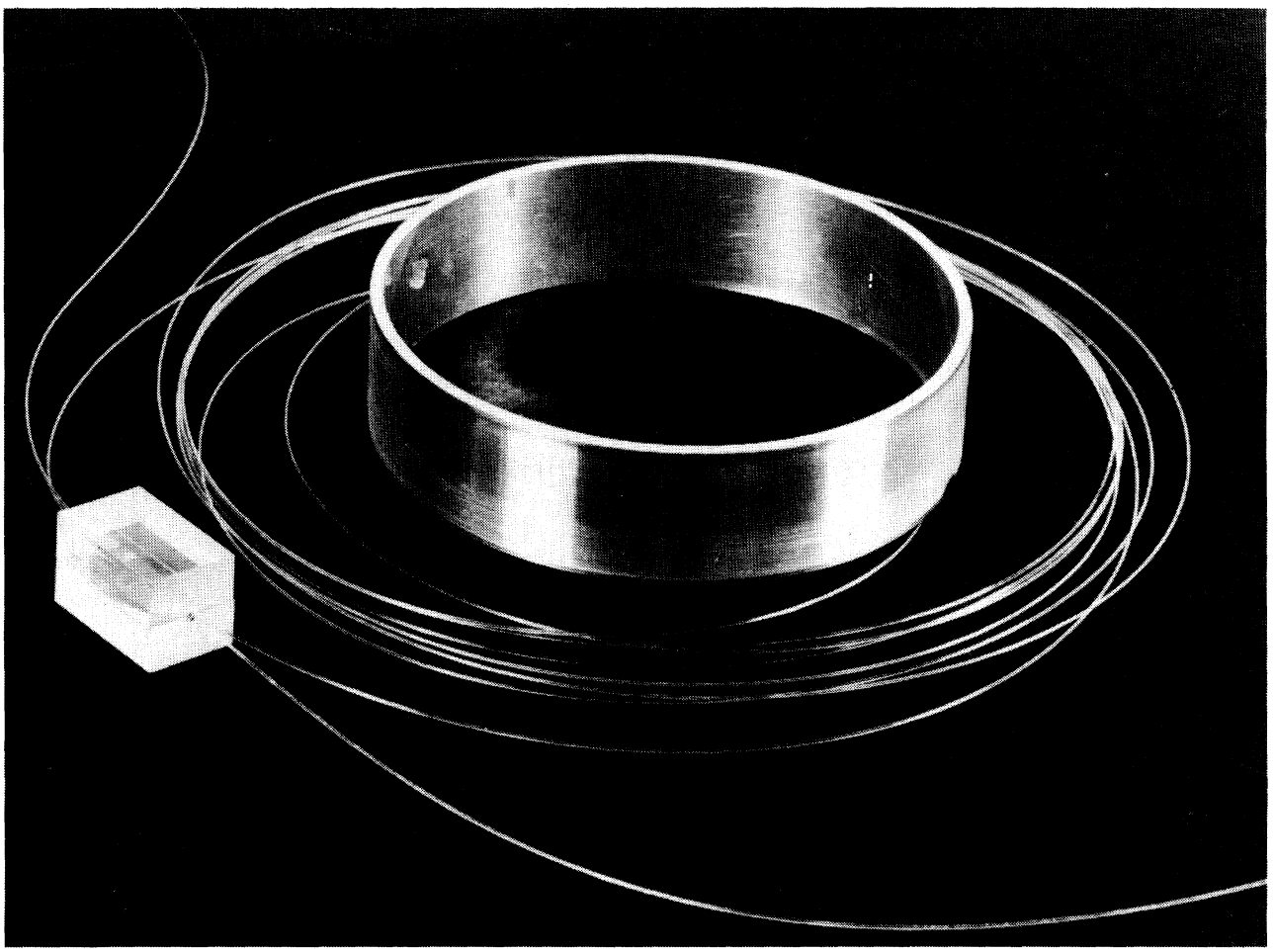

Figure 4. Spliced resonant ring #2.

5. DISCUSSION & CONCLUSION

It can be concluded from calculations of ρ^2 that the average splice loss for #1 is ≈-0.16 dB, which is above what was expected. From Table 3, optimum CR is calculated to be 89.7 percent, which is within the adjustment range of coupler #1. The adjustable resonator could just as well have been assembled in the single-strand configuration due to the extra loss.

The OCB resonator had lossy splices as well (≈-0.14 dB), which was fortunate to get deep dips. This ring is currently being evaluated in an resonant fiber-optic gyro (RFOG) system. Effects of the splices in the cavity on backreflection, dip symmetry as a function of topology, and the relationship of orthogonal polarization dip to coil extinction ratio will be investigated.[22] Optimization of the design and construction is being undertaken to reduce the linewidth of the assemblies.

In conclusion, moderate finesse hybrid PM/PZ resonators have been demonstrated and are being applied to possible RFOG applications. It is hoped that coil and coupler losses can be reduced to <<-0.1 dB; splice loss will dominate the loop losses. The mode-field diameter of PM and PZ fibers was measured to be 9.8 μm and 8.6 μm, respectively. The minimum theoretical loss for these fibers is calculated to be on the order of -0.07 dB.[23] As design of components is optimized and splice loss is further reduced, finesse on the order of 100 would be achievable for loop losses of about -0.14 dB.

ACKNOWLEDGMENTS

Robert E. Sutherland is presently employed at Micracor, Inc., Comtech Park, 696 Virginia Road, Concord, MA 01742. The authors would like to acknowledge K. Champagne for performing the splicing, and S. Root for coupler preparation.

REFERENCES

1. R. Dahlgren, "Lapped Polarization-Maintaining Fiber Resonator," *Optical Fiber Sensors '88*, 2, Part 1, 29-37, 1988.

2. C. Yue, J. Peng, Y. Liao, and B. Zhou, "Fibre Ring Resonator with Finesse of 1260," *Elect. Lett.*, 24(10), 622-3, 1988.

3. K. Iwatsuki, K. Hotate, and M. Higashiguchi, "Eigenstate of Polarization in a Fiber Ring Resonator and Its Effect in an Optical Passive Ring-Resonator Gyro," *Appl. Opt.*, 25(15), 2606-2612, 1986.

4. P. Mouroulis, "Polarization Fading Effects in Polarization-Preserving Fiber Ring Resonators," *Fiber Optic and Laser Sensors VII*, 1169, 400-412, 1989.

5. R. E. Meyer, S. Ezekiel, D. J. Stowe, and V. J. Tekippe, "Passive Fiber-Optic Ring Resonator for Rotation Sensing," *Optics Letters*, V. 8, No. 12, p. 644, 1983.

6. R. Carroll, "Polarization Crosstalk in a PM Fiber Resonator Gyro," *Fiber Optic and Laser Sensors VII*, 1169, 388-399, 1989.

7. G. A. Sanders, R. B. Smith, and G. F. Rouse, "Novel Polarization-Rotating Fiber Resonator for Rotation Sensing Applications," *Fiber Optic and Laser Sensors VII*, 1169, 3732-381, 1989.

8. M. V. Andres and K. W. H. Foulds, "Optical-Fiber Resonant Rings Based on Polarization-Dependent Couplers," *JLWT*, 8(8), 1212-1220, 1990.

9. U.S. Patent #4,991,922, "Optical Fiber Coupler & Method."

10. S. L. A. Carrara, B. Y. Kim, and H. J. Shaw, "Elasto-Optic Alignment of Birefringent Axes in Polarization-Holding Optical Fiber," *Opt. Lett.* 11(7), 470-472, 1986.

11. A. Lindquist, "Pitch, Polytron, and Polyurethane: A Comparison," *Appl. Opt.*, 25(21), 3796-3797, 1986.

12. M. J. F. Diggonet, J. R. Feth, and L. F. Stokes, "Measurement of the Core Proximity in Polished Fiber Substrates and Couplers," *Opt. Lett.*, 10(9), 463-465, 1985.

13. J. M. Bennett and L. Mattsson, "Cleaning and Inspection of Surfaces," *Surface Roughness and Scattering*, Chapter 8, Optical Society of America, 1990 .

14. L. Rayleigh, "A Study of Glass Surfaces in Optical Contact," *Proc. Roy. Soc. A*, 156, 326-349, 1936.

15. S. S. Kachkin and Y. V. Lisitsyn, "Optical-Contact Bonding Strength of Glass Components," *Sov. J. Opt. Tech.*, 47(3), 159-161, 1980.

16. K. Okamoto, "Single-Polarization Operation in Highly Birefringent Optical Fibers," *Appl. Opt.*, 23(15), 2638-2642, 1984.

17. F. A. Burton and S. A. Cassidy, "Theory and Measurement of Mode Coupling and Loss in Waveguide Polarizers," *Integrated Photonics Research*, 5, 15, 1990.

18. F. M. Sears, "Polarization-Maintenance Limits in Polarization Maintaining Fiber & Measurements," *JLWT*, Vol. 8, No. 5, p. 684.

19. U.S. Patent #5,022,735, "Fiber Splice Coating System."

20. R. Carroll, C. D. Coccoli, D. Cardarelli, and G. T. Coate, "The Passive Resonator Fiber Optic Gyro and Comparison to the Interferometer Fiber Gyro," *Fiber Optic Gyros: 10th Anniversary Conference*, 719, 169-177, 1986.

21. R. Dahlgren, and O. Laznicka, "Ultra-High Finesse Polarization-Maintaining Fiber Resonator," *Fiber Optic and Laser Sensors VII*, 1169, 382-387, 1989.

22. R. Carroll, to be published.

23. D. Marcuse, "Loss Analysis of Single-Mode Fiber Splices," *BSTJ*, 56(5), 703-719, 1977.